Inorg. Chem. **2007**, *46*, 5381–5389

Synthesis, Structure, Redox Properties, and Catalytic Activity of New Ruthenium Complexes Containing Neutral or Anionic and Facial or Meridional Ligands: An Evaluation of Electronic and Geometrical Effects

Isabel Serrano,[†] Xavier Sala,[†] Elena Plantalech,[†] Montserrat Rodríguez,[†] Isabel Romero,*[,†] Susanna Jansat,[‡] Montserrat Gómez,[‡] Teodor Parella,[§] Helen Stoeckli-Evans,[||] Xavier Solans,[⊥] Mercè Font-Bardia,[⊥] Balamurugan Vidjayacoumar,[#] and Antoni Llobet*[,+]

Departament de Química, Universitat de Girona, Campus de Montilivi, E-17071 Girona, Spain, Departament de Química Inorgànica, Departament de Cristal·lografia, Mineralogia i Dipòsits Minerals, Universitat de Barcelona, Martí i Franquès 1−11, 08028 Barcelona, Spain, Departament de Química i Servei de RMN, Universitat Autònoma de Barcelona, Bellaterra, E-08193 Barcelona, Spain, Institute of Chemistry, University of Neuchatel, Av. Bellevaux 51, CH-2000 Neuchatel, Switzerland, University of Ottawa, Ottawa, Ontario K1N 6N5, Canada, and Institute of Chemical Research of Catalonia (ICIQ), Av. Països Catalans 16, 43007 Tarragona, Spain

Received January 18, 2007

The synthesis of a family of new Ru complexes containing meridional or facial tridentate ligands with the general formula $[Ru^{II}(T)(D)(X)]^{n+}$ [T = 2,2′:6′,2″-terpyridine or tripyrazolylmethane; D = 4,4′-dibenzyl-4,4′,5,5′-tetrahydro-2,2′-bioxazole (*S*,*S*-box-C) or 2-[((1′*S*)-1′-(hydroxymethyl)-2′-phenyl)ethylcarboxamide]-(4*S*)-4-benzyl-4,5-dihydrooxazole (*S*,*S*-box-O); X = Cl, H_2O, MeCN or pyridine] has been described. All complexes have been spectroscopically characterized in solution through ^1H NMR and UV–vis techniques. Furthermore, all of the chloro complexes presented here have also been characterized in the solid state through monocrystal X-ray diffraction analysis. The oxazolinic *S*,*S*-box-C ligands undergo a Ru-assisted hydrolysis reaction generating the corresponding amidate anionic oxazolinic ligands *S*,*S*-box-O, which are also strongly attached to the metal center and produce a strong σ-donation effect over the Ru metal center. The redox properties of all complexes have also been studied by means of cyclic voltammetry, strongly reflecting the nature of the ligands; both effects, geometrical (facial vs meridional) and electronic (neutral vs anionic), can be unveiled and rationalized. Finally, the reactivity of the $Ru–OH_2$ complexes has been tested with regard to the epoxidation of *trans*-stilbene, and it has been shown that, in this particular case, the reactivity is practically not dependent on the redox potentials of the catalyst but, in sharp contrast, it is strongly dependent on the geometry of the tridentate ligands.

Introduction

In the field of redox catalysis, the relationship between the catalyst performance and the catalyst structure is further complicated by the presence of multiple redox states that need to be cycled through the different transition-metal complex species involved in the catalytic cycle. Therefore, the thermodynamic and kinetic characterization of the reactions that undergo the different oxidation state species of a catalyst is of paramount importance in this field. Redox properties for a given transition metal can be, in principle, tuned through the nature of the ligands bonded to the metal center.[1] To this end, Lever introduced a parameter associated

* To whom correspondence should be addressed. E-mail: marisa.romero@udg.es (I.R.), allobet@ICIQ.es (A.L.).
[†] Universitat de Girona.
[‡] Institute of Chemical Research of Catalonia (ICIQ) and Departament de Química, Universitat Autònoma de Barcelona.
[§] Servei de RMN, Universitat Autònoma de Barcelona.
[||] University of Neuchatel.
[⊥] Departament de Cristal·lografia, Mineralogia i Dipòsits Minerals, Universitat de Barcelona.
[#] University of Ottawa.
[+] Departament de Química, Universitat Autònoma de Barcelona.

(1) Szczepura, L. F.; Maricich, S. M.; See, R. F.; Churchill, M. R.; Takeuchi, K. J. *Inorg. Chem.* **1995**, *34*, 4198.

10.1021/ic070087q CCC: $37.00
Published on Web 05/19/2007

Chart 1. Drawings of Ligands

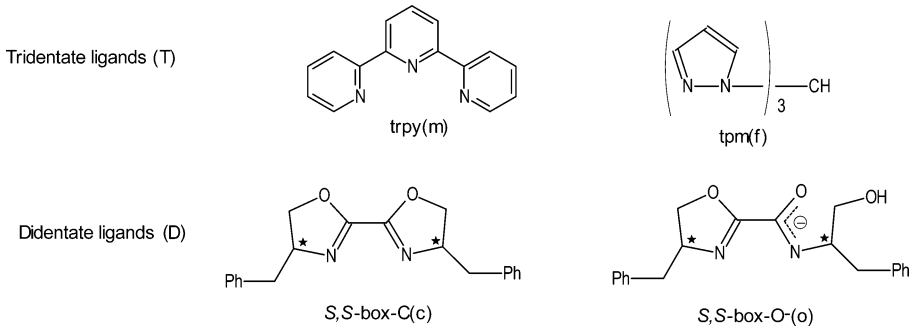

with a particular ligand, named E_L, in order to attempt to predict the $E°$ redox potential of a given $M^{n+}/M^{(n-1)+}$ redox couple.[2] Lever equations work roughly well for complexes that present only one accessible oxidation state. In particular, the Ru^{III}/Ru^{II} redox potential for the octahedral RuN_6 type of polypyridylic complexes is a remarkably well-suited example. The Lever parameter is defined as the summation of individual E_L values for each ligand attached to the metal center but does not take into account the geometrical situation of the ligands involved and does not contemplate also the possibility of multiple electron-transfer processes.[3] The prediction of redox potentials for complexes undergoing multiple electron-transfer processes can only be done through empirical types of correlations, such as the Meyer−Lever correlation described recently.[2,3] The detailed knowledge of the electronic structure of a transition-metal complex at different oxidation states would allow the prediction/calculation of meaningful redox potentials. At present, the available computational tools that could perform such a task in a reasonably cost-efficient manner are based on density functional theory (DFT) methods. However, the results obtained so far using DFT calculations can be considered at their infancy and are certainly far from being accurate.[4]

Therefore, there is a need for a sufficiently large body of complexes with different geometric options and/or multiple oxidation states in which empirical correlations can be established and theoretical methods checked.

Ruthenium polypyridyl complexes have been extensively studied over the years because they enjoy a combination of unique chemical, electrochemical, and photochemical properties[5] that has allowed exploration of a wide variety of fields including photochemistry and photophysics,[6] bioinorganics,[7] and catalysis.[8] In particular, $Ru-H_2O$ complexes with N-based ligands have been investigated in order to develop new catalysts for both organic and inorganic oxidation processes. For oxidative processes, the Ru−oxo group is mainly the active species for this type of chemistry and has been shown to be able to oxidize a variety of substrates, including, among others, alcohols, alkenes,[9,10] or even alkanes.[11] Oxazoline-containing ligands have been shown to be a convenient type of ligand because of their easy synthetic accessibility, modular nature, and applicability in a wide range of metal-catalyzed transformations.[12−14]

In the present paper, we report the synthesis, structure, and redox properties of a new family of Ru complexes containing neutral and anionic oxazolinic ligands together with the facial and meridional N-based ligands shown in Chart 1.

This combination of ligands has allowed us to observe and quantify both electronic and geometrical effects. Furthermore, we also report the influence of those properties on the Ru complexes over their reactivity with regard to the epoxidation of *trans*-stilbene (TS).

Experimental Section

Materials. All reagents used in the present work were obtained from Aldrich Chemical Co. and were used without further purification. Reagent-grade organic solvents were obtained from SDS, and high-purity deionized H_2O was obtained by passing distilled H_2O through a nanopure Milli-Q water purification system. $RuCl_3 \cdot 2H_2O$ was supplied by Johnson and Matthey Ltd. and was used as received.

(2) Lever, A. B. P. *Inorg. Chem.* **1990**, *29*, 1271.
(3) Masllorens, E.; Rodriguez, M.; Romero, I.; Roglans, A.; Parella, T.; Benet-Buchholz, J.; Poyatos, M.; Llobet, A. *J. Am. Chem. Soc.* **2006**, *128*, 5306.
(4) Cramer, C. J. In *Essentials of Computational Chemistry*; John Wiley and Sons Ltd.: New York, 2002; pp 379−381.
(5) (a) Lappin, A. G.; Marusak, R. A. *Coord. Chem. Rev.* **1991**, *109*, 125. (b) Griffith. W. P. *Chem. Soc. Rev.* **1992**, *21*, 179. (c) Wing-Sze Hui, J.; Wong, W.-T. *Coord. Chem. Rev.* **1998**, *172*, 389. (d) Clarke, M. J. *Coord. Chem. Rev.* **2002**, *232*, 69. (e) Meyer, T. J.; Huynh, M. H. V. *Inorg. Chem.* **2003**, *42*, 8140.
(6) (a) *Organic and Inorganic Photochemistry*; Ramamurthy, V., Schanze, K. S., Eds.; Marcel Dekker: New York, 1998. (b) Thompson, D. W.; Schoonover, J. R.; Graff, D. K.; Fleming, C. N.; Meyer, T. J. *J. Photochem. Photobiol. A: Chemistry* **2000**, *137*, 131. (c) Toma, H. E.; Serrasqueiro, R. M.; Rocha, R. C.; Demets, G. J. F.; Winnischofer, H.; Araki, K.; Ribeiro, P. E. A.; Donnici, C. L. *J. Photochem. Photobiol. A: Chemistry* **2000**, *135*, 185. (d) Keefe, M. H.; Benkstein, K. D.; Hupp, J. T. *Coord. Chem. Rev.* **2000**, *205*, 201. (e) Romero, M. I.; Rodríguez, M.; Llobet, A.; Collomb-Dunand-Sauthier, M. N.; Deronzier, A.; Parella, T.; Stoeckli-Evans, H. *J. Chem. Soc., Dalton Trans.* **2000**, 1689. (f) Balzani, V.; Juris, A. *Coord. Chem. Rev.* **2001**, *211*, 97. (g) Dattelbaum, D. M.; Hartshorn, C. M.; Meyer, T. J. *J. Am. Chem. Soc.* **2002**, *124*, 4938. (h) Nikolau, S.; Toma, H. E. *J. Chem. Soc., Dalton Trans.* **2002**, 352. (i) Sala, X.; Romero, I.; Rodríguez, M.; Llobet, A.; Gonzàlez, G.; Martínez, M.; Parella, T.; Benet-Buchholz, J. *Inorg. Chem.* **2004**, *43*, 5403.
(7) (a) Kelly, S. O.; Barton, J. K. *Science* **1999**, *238*, 375. (b) Hall, D. B.; Holmlin, R. E.; Barton, J. K. *Nature* **1996**, *384*, 731. (c) Burrows, C. J.; Muller, J. G. *Chem. Rev.* **1998**, *98*, 1109. (d) Schuster, G. B. *Acc. Chem. Res.* **2000**, *33*, 253. (e) Weatherly, S. C.; Yang, I. V.; Thorp, H. H. *J. Am. Chem. Soc.* **2001**, *123*, 1236.
(8) (a) Murahashi, S. I.; Takaya, H.; Naota, T. *Pure Appl. Chem.* **2002**, *74*, 19. (b) Naota, T.; Takaya, H.; Murahashi, S.-I. *Chem. Rev.* **1998**, *98*, 2599. (c) Rodríguez, M.; Romero, I.; Llobet, A.; Deronzier, A.; Biner, M.; Parella, T.; Stoeckli-Evans, H. *Inorg. Chem.* **2001**, *40*, 4150. (d) Jauregui-Haza, U. J.; Dessoudeix, M.; Kalck, Ph.; Wilhelm, A. M.; Delmas, H. *Catal. Today* **2001**, *66*, 297.

Preparations. Ligands (see Chart 1) *S*,*S*-box-C[15] (4,4′-dibenzyl-4,4′,5,5′-tetrahydro-2,2′-bioxazole) and tpm (tripyrazolylmethane)[16] and the complexes $[Ru^{III}Cl_3(trpy)]$[17] (**1m**; trpy is 2,2′:6′,2″-terpyridine) and $[Ru^{III}Cl_3(tpm)]$[18] (**1f**) were prepared as described in the literature. All synthetic manipulations were routinely performed under a N_2 atmosphere using Schlenk tubes and vacuum-line techniques. Electrochemical experiments were performed under either a N_2 or Ar atmosphere with degassed solvents.

$[Ru^{II}Cl(box\text{-}C)(trpy)](PF_6)\cdot C_4H_{10}O$ (2mc·$C_4H_{10}O$) and $[Ru^{II}Cl(box\text{-}O)(trpy)]\cdot C_4H_{10}O$ (2mo·$C_4H_{10}O$). A sample of **1m** (400 mg, 0.91 mmol) was added to a 100 mL round-bottomed flask containing a solution of LiCl (55 mg, 1.29 mmol) dissolved in 80 mL of EtOH/H_2O (3:1), under magnetic stirring. Then NEt_3 (0.21 mL) was added, and the reaction mixture was stirred at room temperature for 30 min. Next *S*,*S*-box-C (291 mg, 0.91 mmol) was added and heated at reflux for 2 h. The hot solution was then filtered off in a frit and the volume reduced to dryness in a rotary evaporator under reduced pressure. Afterward the solid obtained was dissolved in CH_2Cl_2 and washed several times with H_2O. The organic phase was then dried over $MgSO_4$ and the volume again reduced to dryness. The solid obtained in this manner was a mixture of complexes **2mc** and **2mo** that can be separated by column chromatography (Al_2O_3; 98:2 CH_2Cl_2/MeOH). The chloro complex **2mc** was then dissolved in MeOH (10 mL), and to this solution was added 1.5 mL of a saturated aqueous solution of $NaPF_6$ (1.5 mL). The volume was reduced to dryness under low pressure, and the solid obtained was then dissolved in CH_2Cl_2 and washed several times with H_2O. The organic phase was then dried over $MgSO_4$ and the volume again reduced to dryness. The solid obtained in this manner was finally recrystallized from a hot mixture of MeOH/ether (1:1). Upon cooling, a black dust was obtained, which was filtered on a frit washed with a small amount of cold MeOH and dried under vacuum. Chloro complex **2mo** was recrystallized from MeOH/ether.

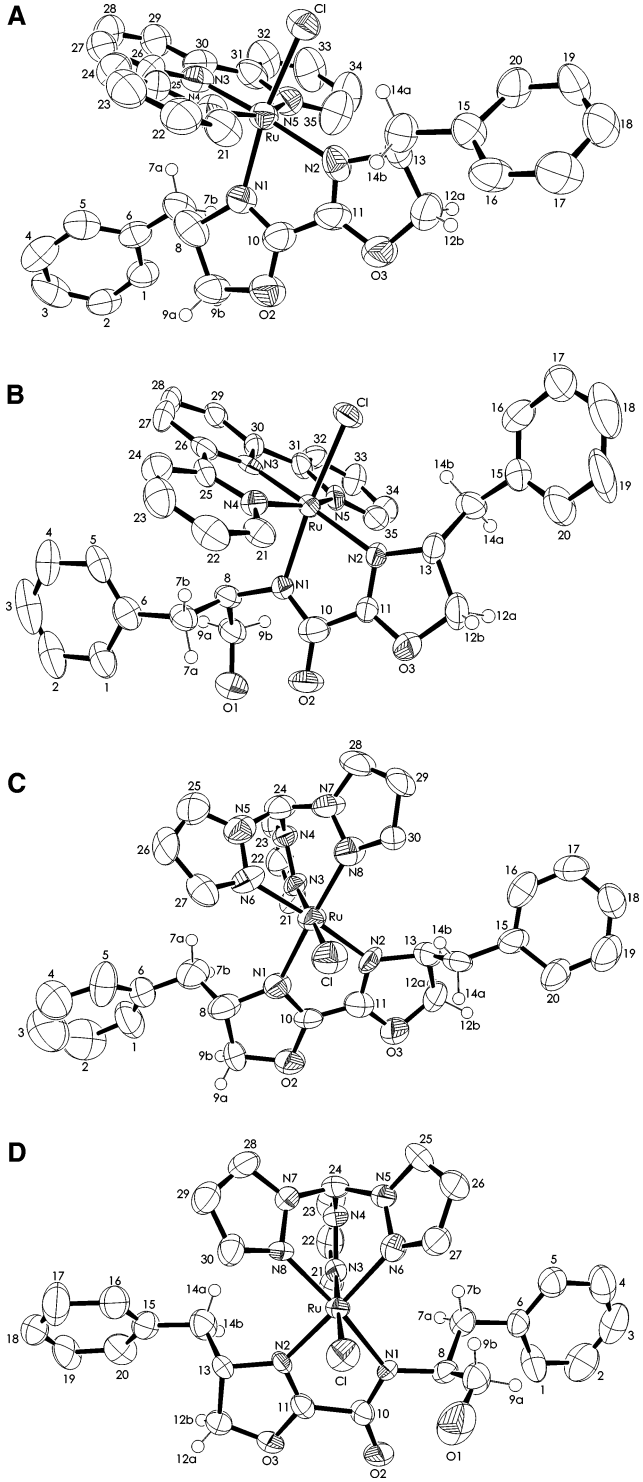

Figure 1. ORTEP view (ellipsoids are drawn at the 50% probability level) of the molecular structure of cation **2mc** (A), neutral complex **2mo** (B), cation **2fc** (C), and neutral complex **2fo** (D), including the atom numbering scheme.

(a) Data for 2mc. Yield: 187 mg (26.4%). Anal. Found (calcd) for $C_{35}H_{31}N_5O_2ClRuPF_6\cdot C_4H_{10}O$: C, 51.52 (51.29); N, 7.70 (7.69);

(9) (a) Thompson, M. S.; Meyer, T. J. *J. Am. Chem. Soc.* **1982**, *104*, 4106. (b) Roecker, L. E.; Meyer, T. J. *J. Am. Chem. Soc.* **1987**, *109*, 746. (c) Marmion, M. E.; Takeuchi, K. J. *J. Am. Chem. Soc.* **1988**, *110*, 1742. (d) Binstead, R. A.; MacGuire, M. E.; Dovletoglou, A.; Seok, W. K.; Roecker, L. E.; Meyer, T. J. *J. Am. Chem. Soc.* **1992**, *114*, 173. (e) Catalano, V. J.; Heck, R. A.; Immoos, C. E.; Ohman, A.; Hill, M. G. *Inorg. Chem.* **1998**, *37*, 2150. (f) Che, C. M.; Cheng, K. W.; Chan, M. C. W.; Lau, T. C.; Mak, C. K. *J. Org. Chem.* **2000**, *65*, 7996. (g) Lau, T. C.; Che, C. M.; Lee, W. O.; Poonl, C. K. *J. Chem. Soc., Chem. Commun.* **1988**, 1406. (h) Jitsukawa, K.; Oka, Y.; Einaga, H.; Masuda, H. *Tetrahedron Lett.* **2001**, *42*, 3467.

(10) (a) Stultz, L. K.; Binstead, R. A.; Reynolds, M. S.; Meyer, T. J. *J. Am. Chem. Soc.* **1995**, *117*, 2520. (b) Fung, W.-H.; Yu, W. Y.; Che, C.-M. *J. Org. Chem.* **1998**, *63*, 7715. (c) Jitsukawa, K.; Oka, Y.; Einaga, H.; Masuda, H. *Tetrahedron Lett.* **2001**, *42*, 3467. (d) Zhang, R.; Yu, W.-Y.; Lai, T.-S.; Che, C.-M. *Chem. Commun.* **1999**, 409. (e) Yu, W.-Y.; Fung, W.-H.; Zhu, J.-L.; Cheung, K.-K.; Ho, K.-K.; Che, C.-M. *J. Chin. Chem. Soc.* **1999**, *46*, 341. (f) Jitsukawa, K.; Shiozaki, H.; Masuda, H. *Tretrahedron Lett.* **2002**, *43*, 1491.

(11) Yamaguchi, M.; Kumano, T.; Masui, D.; Yamagishi, T. *Chem. Commun.* **2004**, 798.

(12) (a) Nishiyama, H.; Itoh, Y.; Matsumoto, H.; Park, S.-B.; Itoh, K. *J. Am. Chem. Soc.* **1994**, *116*, 2223. (b) Jiang, Y.; Jiang, Q.; Zhang, X. *J. Am. Chem. Soc.* **1998**, *120*, 3817. (c) Braunstein, P.; Fryzuk, M. D.; Naud, F.; Rettig, S. J. *J. Chem. Soc., Dalton Trans.* **1999**, 589. (d) Burguete, M. I.; Fraile, J. M.; García, J. I.; García-verdugo, E.; Luis, S. V.; Mayoral, J. A. *Org. Lett.* **2000**, *2*, 3905. (e) Ostergaard, N.; Jensen, J. F.; Tanner, D. *Tetrahedron* **2001**, *57*, 6083. (f) McManus, H. A.; Guiry, P. J. *Chem. Rev.* **2004**, *104*, 4151. (g) Le Maux, P.; Abrunhosa, I.; Berchel, M.; Simonneaux, G.; Gulea, M.; Masson, S. *Tetrahedron: Asymmertry* **2004**, *15*, 2569. (h) Tse, M. K.; Klawonn, M.; Bhor, S.; Döbler, C.; Anilkumar, G.; Hugl, H.; Mägerlein, W.; Beller, M. *Org. Lett.* **2005**, *7*, 987.

(13) (a) Hua, X.; Shang, M.; Lappin, A. G. *Inorg. Chem.* **1997**, *36*, 3735. (b) Gomez, M.; Muller, G.; Rocamora, M. *Coord. Chem. Rev.* **1999**, *193*−*195*, 769. (c) Nishiyama, H.; Park, S.-B.; Haga, M.-A.; Aoki, K.; Itoh, K. *Chem. Lett.* **1994**, 1111.

(14) Rechavi, D.; Lemaire, M. *Chem. Rev.* **2002**, *102*, 3467.

(15) Bolm, C.; Weickhardt, K.; Zehnder, M.; Glasmacher, D. *Chem. Ber.* **1991**, *124*, 1173.

(16) Huckel, W.; Bretschneider, H. *Ber. Chem.* **1937**, *9*, 2024.

(17) Sullivan, B. P.; Calvert, J. M.; Meyer, T. J. *Inorg. Chem.* **1980**, *19*, 1404.

(18) Llobet, A.; Doppelt, P.; Meyer, T. J. *Inorg. Chem.* **1998**, *27*, 514.

Table 1. Crystal Data for Complexes **2mc**, **2mo**, **2fc**, and **2fo**

	2mc	**2mo**	**2fc**	**2fo**
empirical formula	$C_{35}H_{31}ClF_6N_5O_2PRu$	$C_{35}H_{32}ClN_5O_3Ru$	$C_{31}H_{32}Cl_3F_4N_8O_2BRu$	$C_{31}H_{35}ClN_8O_4Ru$
fw	835.14	706.67	842.23	720.19
cryst syst	orthorhombic	orthorhombic	monoclinic	orthorhombic
space group	$P2_12_12_1$	$P2_12_12_1$	$C2$	$P2_12_12_1$
a, Å	9.8992(10)	12.4474(11)	17.214(1)	9.6930
b, Å	17.4573(14)	16.2194(12)	10.278(1)	15.2380
c, Å	22.946(2)	31.9140(18)	19.579(1)	22.321
α, deg	90	90	90	90
β, deg	90	90	97.9620(10)	90
γ, deg	90	90	90	90
V, Å^3	3965.4(6)	6443.1(8)	3430.6(4)	3296.9(5)
formula units/cell	4	4	2	4
temp, K	223(2)	223(2)	293(2)	293(2)
λ(Mo Kα), Å	0.71073	0.71073	0.71069	0.71069
ρ_{calcd}, g cm^{-3}	1.399	1.457	1.550	1.451
R1[a]	0.0797	0.0641	0.0547	0.0539
wR2[b]	0.1959	0.1518	0.1122	0.1334

[a] $R1 = \sum||F_o| - |F_c||/\sum|F_o|$. [b] $wR2 = [\sum\{w(F_o^2 - F_c^2)^2\}/\sum\{w(F_o^2)^2\}]^{1/2}$, where $w = 1/[\sigma^2F_o^2 + (0.0377P)^2 + 1.65P]$ and $P = (F_o^2 + 2F_c^2)/3$.

H, 4.54 (4.67). $E_{1/2}(CH_3CN) = 0.79$ V vs SSCE. UV−vis (CH_2Cl_2): λ_{max}, nm (ϵ, M^{-1} cm^{-1}) 276 (19 700), 318 (27 200), 378 (3970), 446 (5500), 502 (8300).

(b) Data for 2mo. Yield: 206 mg (32%). Anal. Found (calcd) for $C_{35}H_{33}N_5O_3ClRu\cdot C_4H_{10}O$: C, 59.95 (59.78); N, 8.96 (9.19); H, 5.42 (5.21). $E_{1/2}(CH_3CN) = 0.27$ V vs SSCE. UV−vis (CH_2Cl_2): λ_{max}, nm (ϵ, M^{-1} cm^{-1}) 278 (24 800), 316 (25 100), 326 (23 700), 386 (9500), 410 (9600), 540 (8050).

For the NMR assignment, we used the same numbering scheme as that for the X-ray structures displayed in Figure 1.

[Ru^{II}(box-C)(trpy)OH$_2$](PF$_6$)$_2$·H$_2$O (3mc·H$_2$O). A sample of $AgPF_6$ (6.3 mg, 0.025 mmol) was added to a solution of acetone/H_2O (1:1; 30 mL) containing **2mc** (150 mg, 0.019 mmol), and the resulting mixture was heated at reflux for 1.5 h. AgCl was filtered off through a frit containing celite and the volume reduced in a rotary evaporator under reduced pressure. The solid obtained was then stirred in H_2O for 1.5 h and filtered and the volume reduced to dryness. The residue obtained was dissolved in acetone and filtered again and the volume reduced to dryness. Yield: 148 mg (91%). Anal. Found (calcd) for $RuC_{35}H_{33}N_5O_3P_2F_{12}\cdot H_2O$: C, 42.8 (42.89); N, 7.14 (7.34); H, 3.60 (3.89). $E_{1/2}$(phosphate buffer pH = 7) = 0.48 and 0.60 V vs SSCE. UV−vis (phosphate buffer pH = 7): λ_{max}, nm (ϵ, M^{-1} cm^{-1}) 272 (18 100), 314 (29 900), 414 (sh), 470 (8500).

[Ru^{II}(box-O)(trpy)OH$_2$](BF$_4$)·H$_2$O (3mo·H$_2$O). A sample of $AgBF_4$ (7.7 mg, 0.040 mmol) was added to a solution of acetone/H_2O (1:1; 40 mL) containing **2mo** (200 mg, 0.028 mmol), and the resulting mixture was heated at reflux for 1.5 h. AgCl was filtered off through a frit containing celite and the volume reduced in a rotary evaporator under reduced pressure. The solid obtained was then stirred in H_2O for 1.5 h and filtered and the volume reduced to dryness. The residue obtained was then dissolved in acetone and filtered again and the volume reduced to dryness. Yield: 189 mg (86%). Anal. Found (calcd) for $C_{35}H_{34}N_5O_4RuBF_4\cdot H_2O$: C, 52.91 (52.89); N, 8.81 (8.90); H, 4.57 (4.75). $E_{1/2}$(phosphate buffer pH = 7) = 0.20 V vs SSCE. UV−vis (phosphate buffer pH = 6): λ_{max}, nm (ϵ, M^{-1} cm^{-1}) 272 (22 600), 322 (26 800), 386 (6200), 500 (6200).

[Ru^{II}(box-O)(CH$_3$CN)(trpy)](PF$_6$)·3H$_2$O (4mo·3H$_2$O). A sample of the aqua complex **3mo** (150 mg, 0.019 mmol) was dissolved in acetonitrile (50 mL) and stirred at room temperature for 3.5 h. Then, a saturated aqueous solution of KPF_6 (1.5 mL) was added, the volume reduced in a rotary evaporator, and the complex precipitated with ether. Yield: 135 mg (82%). Anal. Found (calcd) for $C_{37}H_{35}N_6O_3RuPF_6\cdot 3H_2O$: C, 48.74 (48.68); N, 9.22 (9.19); H, 4.53 (4.69). $E_{1/2}(CH_3CN) = 0.69$ V vs SSCE. UV−vis (CH_3CN): λ_{max}, nm (ϵ, M^{-1} cm^{-1}) 272 (19 100), 316 (24 500), 374 (5500), 482 (5150).

[Ru^{II}(box-O)(py)(trpy)](PF$_6$)·H$_2$O (5mo·H$_2$O). A sample of neat pyridine (2 mL, 24.7 mmol) was added to **3mo** (200 mg, 0.026 mmol) dissolved in MeOH (50 mL). The resulting solution was magnetically stirred at room temperature for 2 days, and then a saturated aqueous solution of KPF_6 (1.5 mL) was added. Then, the volume was reduced under reduced pressure and the complex precipitated with ether. Yield: 120 mg (52%). Anal. Found (calcd) for $C_{40}H_{37}N_6O_3RuPF_6\cdot H_2O$: C, 52.58 (52.49); N, 9.20 (9.19); H, 4.30 (4.31). $E_{1/2}(CH_3CN) = 0.67$ V vs SSCE. UV−vis (CH_2Cl_2): λ_{max}, nm (ϵ, M^{-1} cm^{-1}) 276 (22 100), 320 (27 600), 360 (9750), 514 (6100).

[Ru^{II}Cl(box-C)(tpm)](BF$_4$)·H$_2$O (2fc·H$_2$O) and [Ru^{II}Cl(box-O)(tpm)]·2CH$_3$OH (2fo·2CH$_3$OH). A sample of **1f** (390 mg, 0.94 mmol) was added to a 100 mL round-bottomed flask containing a solution of LiCl (90 mg, 2.06 mmol) in EtOH/H_2O (3:1; 80 mL), under magnetic stirring. Then, NEt_3 (0.26 mL) was added and the reaction mixture stirred at room temperature for 30 min, at which point *S*,*S*-box-C (300 mg, 0.94 mmol) was added and then the resulting mixture was heated at reflux for 2 h. The hot solution was filtered off in a frit and the volume reduced to dryness in a rotary evaporator under reduced pressure. The solid obtained was then dissolved in CH_2Cl_2 and washed several times with H_2O. The organic phase was then dried over $MgSO_4$ and the volume again reduced to dryness. The solid obtained in this manner was a mixture of complexes **2fc** and **2fo**, which were separated by column chromatography (alumina; 95:5 CH_2Cl_2/MeOH). Chloro complex **2fc** was dissolved in MeOH (10 mL), and a saturated aqueous solution of $NaBF_4$ (1.5 mL) was added. The red solid obtained was filtered off in a frit and then dissolved in CH_2Cl_2. The volume was evaporated under reduced pressure to dryness. The solid obtained in this manner was then recrystallized from a hot mixture of CH_2Cl_2/ether (1:1). Chloro complex **2fo** was recrystallized in a MeOH/diethyl oxide solution.

(a) Data for 2fc. Yield: 150 mg (21.1%). Anal. Found (calcd) for $C_{30}H_{30}N_8O_2ClRuBF_4\cdot H_2O$: C, 46.44 (46.37); N, 14.44 (14.12); H, 4.16 (4.04). $E_{1/2}(CH_2Cl_2) = 0.83$ V vs SSCE. UV−vis (CH_2Cl_2): λ_{max}, nm (ϵ, M^{-1} cm^{-1}) 271 (9900), 326 (7200), 468 (6400).

(b) Data for 2fo. Yield: 30 mg (4.5%). Anal. Found (calcd) for $C_{30}H_{31}N_8O_3ClRu\cdot 2CH_3OH$: C, 51.10 (51.14); N, 14.9 (14.68); H,

Scheme 1. Synthetic Pathways and Labeling Scheme for Complexes Described in This Work

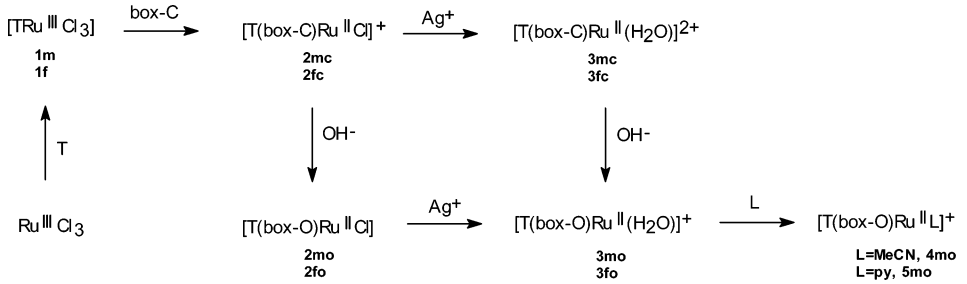

5.23 (4.90). $E_{1/2}(CH_2Cl_2) = 0.24$ V vs SSCE. UV−vis (CH_2Cl_2): λ_{max}, nm (ϵ, M^{-1} cm^{-1}) 270 (6900), 335 (sh), 388 (8600).

[Ru^{II}(box-C)(tpm)OH$_2$](BF$_4$)$_2$·6H$_2$O (3fc·6H$_2$O). A sample of $AgBF_4$ (7.7 mg, 0.040 mmol) was added to a solution of acetone/H_2O (1:1; 15 mL) containing **2fc** (23 mg, 0.030 mmol), and the resulting mixture was heated at reflux for 1.5 h. AgCl was filtered off through a frit containing celite and the volume reduced in a rotary evaporator under reduced pressure. The volume was evaporated under reduced pressure until a brown precipitate was formed. The solid obtained was filtered through a frit, washed with cold H_2O, and dried with ether. Yield: 19 mg (75.5%). Anal. Found (calcd) for $C_{30}H_{32}N_8O_3RuB_2F_8$·$6H_2O$: C, 38.52 (38.69); N, 11.98 (11.58); H, 4.74 (4.41). $E_{1/2}$(phosphate buffer pH = 7) = 0.38 V vs SSCE. UV−vis (phosphate buffer pH = 7): λ_{max}, nm (ϵ, M^{-1} cm^{-1}) 263 (9800), 310 (sh), 423 (4150).

[Ru^{II}(box-O)(tpm)OH$_2$](BF$_4$)·3H$_2$O, 3fo·3H$_2$O. A sample of $AgBF_4$ (17.4 mg, 0.09 mmol) was added to a mixture of MeOH/H_2O (1:1; 15 mL) containing **2fo** (44 mg, 0.064 mmol), and the resulting mixture was heated at reflux for 1 h. AgCl was filtered off through a frit containing celite and the volume reduced in a rotary evaporator under reduced pressure. The solid obtained was then stirred in H_2O for 1.5 h and filtered and the volume reduced to dryness. The residue obtained was dissolved in acetone and filtered again and the volume reduced to dryness. Yield: 19.2 mg (40%). Anal. Found (calcd) for $C_{30}H_{33}N_8O_4RuBF_4$·$3H_2O$: C, 44.4 (44.73); N, 13.81 (13.78); H, 4.84 (4.70). $E_{1/2}$(phosphate buffer pH = 7) = 0.17 and 0.37 V vs SSCE. UV−vis (phosphate buffer pH = 7): λ_{max}, nm (ϵ, M^{-1} cm^{-1}) 260 (6200), 330 (5250), 387 (sh).

Instrumentation and Measurements. IR spectra were recorded on a Mattson Satellite FT-IR with KBr pellets or using a MKII Golden Gate Single Reflection ATR system. UV−vis spectroscopy was performed in a Cary 50 Scan (Varian) UV−vis spectrophotometer with 1 cm quartz cells. pH measurements were done using a Micro-pH-2000 from Crison. Cyclic voltammetric (CV) experiments were performed in a PAR 263A EG&G potentiostat or in a IJ-Cambria ICH-660 potentiostat using a three-electrode cell. Glassy carbon disk electrodes (3 mm diameter) from BAS were used as the working electrode, platinum wire as the auxiliary electrode, and SSCE as the reference electrode (unless explicitly mentioned in the text, the potentials given are always with regard to this reference electrode). All cyclic voltammograms presented in this work were recorded at a 100 mV s^{-1} scan rate under a N_2 atmosphere unless explicitly mentioned. The complexes were dissolved in previously degassed solvents containing the necessary amount of supporting electrolyte to yield a 0.1 M ionic strength solution. In acetonitrile and dichloromethane, (n-Bu_4N)(PF_6) (TBAH) was used as the supporting electrolyte. In aqueous solutions, the pH was adjusted from 0 to 2 with HCl. Potassium chloride was added to keep a minimum ionic strength of 0.1 M. From pH = 2−10, 0.1 M phosphate buffers were used, and from pH = 10−12, diluted, CO_2-free NaOH was used. All $E_{1/2}$ values reported in this work were estimated from CV as the average of the oxidative and reductive peak potentials, ($E_{p,a} + E_{p,c}$)/2. Unless explicitly mentioned, the concentration of the complexes was approximately 1 mM. Bulk electrolyses were carried out in a three-compartment cell using carbon felt from SOFACEL as the working electrode.

^{1}H NMR spectroscopy was carried out on a Bruker DPX 200 MHz or a Bruker 500 MHz spectrometer. Samples were run in acetone-d_6 or dimethyl sulfoxide-d_6 (DMSO-d_6), with internal references (residual protons and/or tetramethylsilane). Elemental analyses were performed using a CHNS−O elemental analyzer EA-1108 from Fisons.

For acid−base spectrophotometric titration, (3−4) × 10^{-5} M buffered aqueous solutions of the complexes were used. The pH of the different solutions was adjusted by adding small volumes (approximately 10 μL) of 4 M NaOH in order to produce a negligible overall volume change. Redox spectrophotometric titrations were performed by sequential addition of a 0.1 M $(NH_4)_2$-[$Ce^{IV}(NO_3)_6$] solution in $HClO_4$ to the complex.

Catalytic Oxidation of *trans*-Stilbene (TS). Experiments have been performed in dichloromethane dried over CaH_2 at room temperature. Iodosylbenzene was prepared by hydrolysis of iodosylbenzene diacetate (Aldrich) in a NaOH solution. In a typical run, Ru catalyst (0.002 mmol), alkene (0.2 mmol), and PhIO or $PhI(OAc)_2$ (0.4 mmol) were stirred at room temperature in dichloromethane (2.5 mL) for 24 h. The end of the reaction was indicated by the disappearance of solid cooxidant. After the addition of an internal standard, an aliquot was taken for gas chromatographic (GC) analysis. The oxidized products were analyzed in a Shimadzu GC-17A gas chromatography apparatus with a TRA-5 column (30 m × 0.25 mm diameter) incorporating a flame ionization detector. GC conditions: initial temperature, 80 °C for 10 min; ramp rate, 10 °C min^{-1}; final temperature, 220 °C; injection temperature, 220 °C; detector temperature, 250 °C; carrier gas, He at 25 mL min^{-1}. All catalytic oxidations were carried out under a N_2 atmosphere.

X-ray Structure Determinations. Suitable crystals of **2mc** and **2mo** were grown by slow diffusion of ether into a CH_2Cl_2 solution as dark-violet blocks, and those of **2fc** and **2fo** were grown by slow diffusion of ether into a MeOH solution as dark-red needles or plates.

(a) Data Collection. Intensity data for **2mo** and **2mc** were collected at 223 K on a Stoe Image Plate Diffraction system using graphite-monochromated Mo Kα radiation.

For crystals **2fc** and **2fo**, intensity data were collected at room temperature on an Enraf-Nonius CAD4 four-circle diffractometer, using graphite-monochromated Mo Kα radiation.

(b) Structure Solution and Refinement. The structures were solved by direct methods using the program *SHELXS-97*.[19a] The

(19) (a) Sheldrick, G. M. SHELXS-97: Program for Crystal Structure Determination. *Acta Crystallogr.* **1990**, *A46*, 467. (b) Sheldrick, G. M. *SHELXL-97*; Universität Göttingen: Göttingen, Germany, 1997.

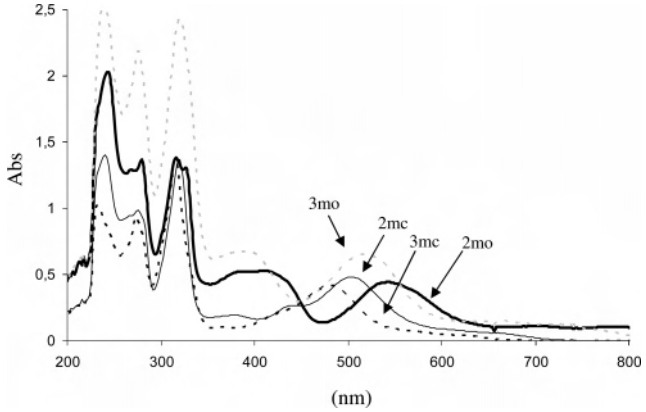

Figure 2. UV−vis spectra for Ru−Cl and Ru−H_2O complexes **2mc**, **2mo**, **3mc**, and **3mo** in CH_2Cl_2.

refinement and all further calculations were carried out using *SHELXL-97*.[19b] The non-H atoms were refined anisotropically, using weighted full-matrix least squares on F^2.

The crystallographic data as well as details of the structures' solution and refinement procedures are reported in Table 1. Supplementary crystallographic data (CIF for **2mc**, **2mo**, **2fc**, and **2fo** have CCDC Nos. 217745, 217744, 631801, and 631802, respectively) can be obtained free of charge via www.ccdc.cam.ac.uk/conts/retrieving.html (or from the Cambridge Crystallographic Data Centre, 12 Union Road, Cambridge CB2 1EZ, U.K.; fax +44 1223 336033 or e-mail deposit@ccdc.cam.ac.uk).

Results and Discussion

Synthesis and Solid-State Structure. The synthetic strategy followed for the preparation of the complexes described in the present paper is outlined in Scheme 1. The trichlororuthenium complexes [$Ru^{III}Cl_3$(trpy)] (**1m**) and [$Ru^{III}Cl_3$(tpm)] (**1f**) are used as starting materials,[16,17] followed by reduction with NEt_3. Then the bisoxazolinic ligand, box-C, is added to form the corresponding monochlororuthenium(II) complexes **2**. For each tridentate ligand, the reaction leads to a mixture of two chloro complexes: **2mc** and **2mo** for the complexes containing the meridional trpy ligand and **2fc** and **2fo** for the complexes containing the facial tpm ligand. The two Ru−Cl complexes obtained in this reaction are the expected **2mc** or **2fc**, where the initial ligand remains intact, but two other complexes are obtained: complex **2mo** and **2fo**, where the oxazolinic ligand has suffered a nucleophilic attack by an OH^- group, leading to ring cleavage and thus generating the new anionic unsymmetric oxazolinic−amidate ligand box-O^- (see Chart 1). These Ru−Cl complexes are easily separated by column chromatography because **2mc** and **2fc** are cationic whereas **2mo** and **2fo** are neutral complexes. Under similar reaction conditions but with no [$TRuCl_3$], the initial box-C ligand does not undergo any chemical transformation, and thus this ring opening is attributed to a Ru-assisted process once the oxazoline ligand is already coordinated due to an enhancement of the iminic C atom electrophilicity. This point is also consistent with the fact that only one type of **2mo** and **2fo** isomer is obtained; given the unsymmetrical nature of the box-O^- ligand, two possible isomers could be obtained in each case. Furthermore, the **2mo**/**2mc** and **2fo**/**2fc** yield ratio can be monitored as a function of the refluxing time, increasing these ratios with increasing time and without any box-O^- ligand isomerization of **2mo** or **2fo** occurring.

It is worth mentioning here that the synthesis of oxazoline compounds is generally carried out under basic conditions[20] and that the oxazolinic rings are highly stable both under basic conditions[21] and in the presence of transition-metal complexes.[22]

The Ru−OH_2 complexes **3** are easily obtained from the corresponding Ru−Cl complexes **2** in the presence of stoichiometric amounts of Ag^+. Finally, the aqua ligand can also be easily replaced by MeCN, **4mo**, or pyridine, **5mo**, as indicated in Scheme 1.

Crystallographic data and selected bond distances and angles for the four Ru−Cl complexes **2** are reported in Table 1 and in the Supporting Information (Table S1). ORTEP views together with their labeling schemes are depicted in Figures 1 and S1 (in the Supporting Information).

In all cases, the Ru metal centers adopt an octahedrally distorted type of coordination where the trpy ligand is bonded in a meridional manner and the tpm ligand in a facial one and the box-C and box-O^- oxazoline ligands act in a didentate fashion. All bond distances and angles are within the expected values for these types of complexes.[23] For the case of **2mo**, the anionic part of the box-O^- ligand is coordinated trans to the Ru−Cl bond; no evidence for the existence of the other possible geometrical isomer has been obtained either in the solid state or in solution.

Delocalization of the carbonyl double bond in amidate types of ligands generates two limiting resonant forms whose structures are represented in the following:

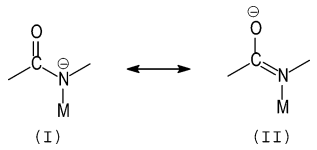

Higher oxidation state complexes favor the resonant form **I**, whereas lower oxidation states favor **II**.[24] X-ray structures of complexes **2fo** and **2mo** present C−O and C−N bond distances (for **2fo**, C10−N1 = 1.308 Å and C10−O2 =

(20) (a) Altenhoff, G.; Goddard, R.; Lehmann, C. W.; Glorius, F. *J. Am. Chem. Soc.* **2004**, *126*, 15195. (b) Sirbu, D.; Consiglio, G.; Milani, B.; Kumar, P. G. A.; Pregosin, P. S.; Gischig, S. *J. Organomet. Chem.* **2005**, *690*, 2254. (c) Desimoni, G.; Faita, G.; Jorgensen, K. A. *Chem. Rev.* **2006**, *106*, 3561. (d) Gómez, M.; Jansat, S.; Muller, G.; Maestro, M. A.; Mahía, J. *Organometallics* **2002**, *21*, 1077. (e) Ghosh, A. K.; Mathivanan, P.; Cappiello, J. *Tetrahedron: Asymmetry* **1998**, *9*, 1.
(21) Arrasate, S.; Lete, E.; Sotomayor, N. *Tetrahedron: Asymmetry* **2001**, *12*, 2077.
(22) Srikanth, A.; Nagendrappa, G.; Chandrasekaran, S. *Tetrahedron* **2003**, *59*, 7761.
(23) Sens, C.; Rodríguez, M.; Romero, I.; Parella, T.; Benet-Buchholz, J.; Llobet, A. *Inorg. Chem.* **2003**, *42*, 8385.
(24) (a) Diaddario, L. L.; Robinson, W. R.; Margerum, D. W. *Inorg. Chem.* **1983**, *22*, 1021. (b) Freeman, H. C.; Taylor, M. R. *Acta Crystallogr.* **1965**, *18*, 939. (c) Freeman, H. C.; Gauss, J. M.; Sinclair, R. L. *J. Chem. Soc., Chem. Commun.* **1968**, 485. (d) Pal, P.; Drew, M. G. B.; Truter, M. R.; Tocher, D. A.; Datta, D. *New J. Chem.* **2003**, *27*, 786. (e) Singh, A. K.; Balamurugan, V.; Mukherjee, R. *Inorg. Chem.* **2003**, *42*, 6497. (f) Patra, A. K.; Ray, M.; Mukherjee, R. *Inorg. Chem.* **2000**, *39*, 652. (g) Beckmann, U.; Bill, E.; Weyhermuller, T.; Wieghardt, K. *Inorg. Chem.* **2003**, *42* (4), 1045.

Table 2. UV−Vis Spectroscopic Features in Aqueous Solution[a] for the Complexes Described in the Present Work

compound	assignment	λ_{max}, nm (ϵ, M^{-1} cm^{-1})
$[Ru^{II}Cl(box\text{-}C)(trpy)](PF_6)$, **2mc**	$\pi \rightarrow \pi^*$	276 (19 700), 318 (27 1200)
	$d\pi \rightarrow \pi^*$	378 (3970), 446 (5500), 502 (8300)
$[Ru^{II}Cl(box\text{-}O)(trpy)]$, **2mo**	$\pi \rightarrow \pi^*$	278 (24 800), 316 (25 100), 326 (23 700)
	$d\pi \rightarrow \pi^*$	386 (9500), 410 (9600), 540 (8050)
$[Ru^{II}(box\text{-}C)(trpy)OH_2](PF_6)_2$, **3mc**	$\pi \rightarrow \pi^*$	272 (18 100), 314 (29 900)
	$d\pi \rightarrow \pi^*$	414 (sh), 470 (8500)
$[Ru^{II}(box\text{-}O)(trpy)OH_2](BF_4)$, **3mo**	$\pi \rightarrow \pi^*$	272 (22 600), 322 (26 800)
	$d\pi \rightarrow \pi^*$	386 (6200), 500 (6200)
$[Ru^{II}(box\text{-}O)(trpy)(py)](PF_6)$, **5mo**	$\pi \rightarrow \pi^*$	276 (22 100), 320 (27 600)
	$d\pi \rightarrow \pi^*$	360 (9760), 514 (6100)
$[Ru^{II}(box\text{-}O)(trpy)(MeCN)](PF_6)$, **4mo**	$\pi \rightarrow \pi^*$	272 (19 100), 316 (24 500)
	$d\pi \rightarrow \pi^*$	374 (5500), 482 (5150)
$[Ru^{II}Cl(box\text{-}C)(tpm)](BF_4)$, **2fc**	$\pi \rightarrow \pi^*$	271 (9900), 326 (7200)
	$d\pi \rightarrow \pi^*$	468 (6400)
$[Ru^{II}Cl(box\text{-}O)(tpm)]$, **2fo**	$\pi \rightarrow \pi^*$	270 (6900), 335 (sh)
	$d\pi \rightarrow \pi^*$	388 (8600)
$[Ru^{II}(box\text{-}C)(tpm)OH_2](BF_4)_2$, **3fc**	$\pi \rightarrow \pi^*$	263 (9800), 310 (sh)
	$d\pi \rightarrow \pi^*$	423 (4150)
$[Ru^{II}(box\text{-}O)(tpm)OH_2](BF_4)$, **3fo**	$\pi \rightarrow \pi^*$	260 (6210), 330 (5250)
	$d\pi \rightarrow \pi^*$	387 (sh)

[a] For the complexes **2mc**, **2mo**, **5mo**, **2fc**, and **2fo**, the spectra were registered in CH_2Cl_2 and in MeCN for complex **4mo**.

1.256 Å; for **2mo**, C10−N1 = 1.317 Å and C10−O2 = 1.270 Å) that are consistent with an intermediate situation and therefore point to a charge delocalization in the NCO backbone.

For the neutral complex **2fo**, it is also of interest to discuss its packing structure. Each Cl ligand of a given complex (see Figure S2 in the Supporting Information) is involved in an intermolecular C−H···Cl hydrogen bonding with the pyrazole (3H) arm of the next molecule in the layer, leading to a 1D single helical architecture along the *b* axis.[25] This helical chain, which also possesses an inner channel running parallel to the helical axis, is further strengthened by the presence of an intramolecular O−H···Cl hydrogen-bonding interaction. The neighboring Ru−Ru distance is 8.771(2) Å.

Spectroscopic Properties. The 1D and 2D NMR spectra of the Ru−Cl (**2mc**, **2mo**, **2fc**, and **2fo**), Ru−H_2O (**3mc**, **3mo**, **3fc**, and **3fo**), Ru−MeCN (**4mo**), and Ru−py (**5mo**) complexes were registered in acetone-d_6 or DMSO-d_6 and are presented and discussed in the Supporting Information. All spectra are consistent with the structures obtained in the solid state.

The UV−vis spectra of complexes **2**−**5** are displayed in Figure 2 and in the Supporting Information, whereas their main features are presented in Table 2. The complexes exhibit ligand-based $\pi-\pi^*$ bands below 350 nm and relatively intense bands above 350 nm assigned mainly to $d\pi-\pi^*$ transitions due to a series of metal-to-ligand charge-transfer (MLCT) transitions.[26] For the Ru−Cl complexes, the MLCT bands are shifted to the red with regard to Ru−OH_2 due to the relative destabilization of the $d\pi$(Ru) levels provoked by the chloro ligand (see Figure 2). A similar band shifting is also observed for the Ru−OH complexes that can be obtained under basic conditions (see Figure S16 in the Supporting Information). In addition and for the same reason, a similar MLCT shifting is also observed when comparing complexes containing the neutral box-C or the anionic box-O^- ligands. For the particular case of the trpy complexes and taking the **3mc** aqua complex as a reference, the replacement of the aqua by Cl (**3mc** vs **2mc** or **3mo** vs **2mo**) or box-C by box-O^- (**3mc** vs **3mo** or **2mc** vs **2mo**) produces a red shift of roughly 30−40 nm. Thus, when both replacements are made, that is, a comparison of complexes **3mc** and **2mo**, the overall red shift is 70 nm. For the tpm complexes, the situation is not as straightforward as with the ones that contain trpy because of the higher energies of the π^* orbitals of the pyrazolyl rings compared to trpy.[27]

A spectrophotometric acid−base titration of the Ru−aqua complex **3mo** (Figure S17 in the Supporting Information) was carried out in order to calculate its pK_a (eq 1), which led to the value of 11.0, giving two isosbestic points at 452 and 522 nm.

$$[Ru^{II}(box\text{-}O)(trpy)(H_2O)]^+ \xrightarrow[pK_{a1}(Ru^{II}) = 11.0]{} [Ru^{II}(box\text{-}O)(trpy)(OH)] + H^+ \quad (1)$$

pK_a values for the Ru^{II} and Ru^{III} oxidation states in the other Ru−aqua complexes, which are discussed in the following section, were extracted from their Pourbaix diagrams (vide infra) and are displayed in Table 3, together with electrochemical information.

Redox Properties. The redox properties of the Ru−aqua complexes described in the present work were investigated by means of CV and coulombimetric techniques and are summarized in Table 3. The redox potentials for the Ru−aqua complexes, **3**, are pH-dependent because of the capacity of the mentioned aqua ligand to lose protons, as has been shown in eq 1. Furthermore, the aqua ligand is also

(25) (a) Balamurugan, V.; Hundal, M. S.; Mukherjee, R. *Chem. Eur. J.* **2004**, *10*, 1683. (b) Laurent, F.; Plantalech, P.; Donnadieu, B.; Jiménez, A.; Hernández, F.; Martínez-Ripoll, M.; Biner, M.; Llobet, A. *Polyhedron* **1999**, *18*, 3321.

(26) Balzani, V.; Juris, A.; Veturi, M. *Chem. Rev.* **1996**, *96*, 759.

(27) Barqawi, K. R.; Llobet, A.; Meyer, T. J. *J. Am. Chem. Soc.* **1988**, *110*, 7751.

Table 3. pK_a and Electrochemical Data (pH = 7) for the Aqua Complexes Described in This Work and Others for Purposes of Comparison

		$E_{1/2}$[b]					
entry	complex[a] (T)(D)Ru−OH_2	III/II	IV/III	ΔE	p$K_{a,II}$	p$K_{a,III}$	ref
1	trpy−bpy	0.49	0.62	130	9.7	1.7	29b
2	**3mc**	0.48	0.60	120	>10	1.8	*d*
3	**3mo**	0.20			11.0	4.4	*d*
4	tpm−bpy	0.40	0.71	310	10.8	1.9	29a
5	**3fc**	0.38			>10	1.5	*d*
6	**3fo**	0.17	0.37	200	11.0	3.9	*d*
7	*trans*-trpy−pic	0.21	0.45	240	10.0	2.0	19
8	*cis*-trpy−pic	0.38	0.56	180	10.0	3.7	19
9	trpy−acac	0.19	0.56	370	11.2	5.2	29b
10	trpy−tmen	0.36	0.59	230	10.8	0.9	29b

[a] T stands for tridentate ligand, whereas D stands for didentate. Ligand abbreviations used are as follows: acac = acetylacetonate; tmen = *N*,*N*,*N*′,*N*′-tetramethylethylenediamine. [b] Redox potentials in V are reported with regard to the SSCE reference electrode. [c] $\Delta E = E_{1/2}$(IV/III) − $E_{1/2}$(III/II) in mV. [d] This work.

responsible for the easy accessibility of higher oxidation states, as shown in the following equation as an example:

$$[Ru^{IV}(box\text{-}C)(trpy)(O)]^{2+} + 1e^- + 1H^+ \rightarrow [Ru^{III}(box\text{-}C)(trpy)(OH)]^{2+} \quad (2)$$

The complete thermodynamic information regarding the Ru−aqua type of complex can be extracted from the Pourbaix diagrams, exhibited in Figure 3 for **3mc** and **3mo** and in the Supporting Information for **3fc** and **3fo**. For complexes **3mc** and **3fc**, the absence of information in the Pourbaix diagram above pH = 10 is due to the fact that at this high pH a hydrolysis of the oxazolinic box-C ligand takes place, forming the corresponding **3fo** and **3mo** complexes as shown in Scheme 1. Table 3 also contains information of other relevant Ru−trpy−aqua and Ru−tpm−aqua complexes previously described in the literature for purposes of comparison.[28] A careful study of Table 3 allows one to reach the following conclusions: (a) As shown in entries 1, 2 and 4, 5, the replacement of a bpy by a box-C ligand produces a decrease of 10 and 20 mV, respectively, of the $Ru^{III/II}$ redox couple because of the lesser electron-withdrawing capacity of the oxazolinic ligand versus the bpy ligand. A parallel effect can be observed when comparing similar complexes but replacing trpy by tpm as shown in entries 1 and 4. (b) Entries 2, 3 and 5, 6 show the cathodic shift produced by the replacement of a neutral box-C ligand with an anionic box-O^- ligand of 280 and 210 mV, respectively, because of stabilization of Ru^{III}.[29] This is about the same magnitude found, when compared to Ru−trpy−bpy in entry 1, for the pic^- and $acac^-$ cases [entries 7 (280) and 9 (300), respectively]. (c) Complexes **3mo** and **3fo** contain amidate ligands that are trans and cis, respectively, to the Ru−aqua group. This geometrical feature also has a strong influence over the redox potentials. In the trans case, the potential is reduced by 290 mV (compare entries 1 and 3), while for the cis case, the reduction is only 230 mV (entries 4 and 6). A similar trend is observed for the Ru−trpy−pic complexes; the trans generates a 280 mV shift, whereas the cis is of only 110 mV. These data illustrate how the electron density is more effectively transmitted to the metal center in a trans fashion than in cis. (d) In all cases, the exchange of an anionic ligand by a neutral ligand slightly affects p$K_{a,II}$ but strongly influences p$K_{a,III}$. This can be interpreted in the sense that the higher the oxidation state, the stronger the σ donation capability provided by the anionic ligand. (e) It is interesting also to observe that strongly σ-donating neutral ligands can also produce a strong cathodic shift on the $Ru^{III/II}$ potential but have a limited effect over p$K_{a,III}$. Indeed, in entry 10, it is shown that, in sharp contrast with the previous anionic cases, p$K_{a,III}$ slightly decreases instead of increasing. (f) The facial tpm ligand produces larger ΔE values, and thus an enhancement of the zone of stability of oxidation state III, with regard to similar complexes but containing the meridional trpy ligand.

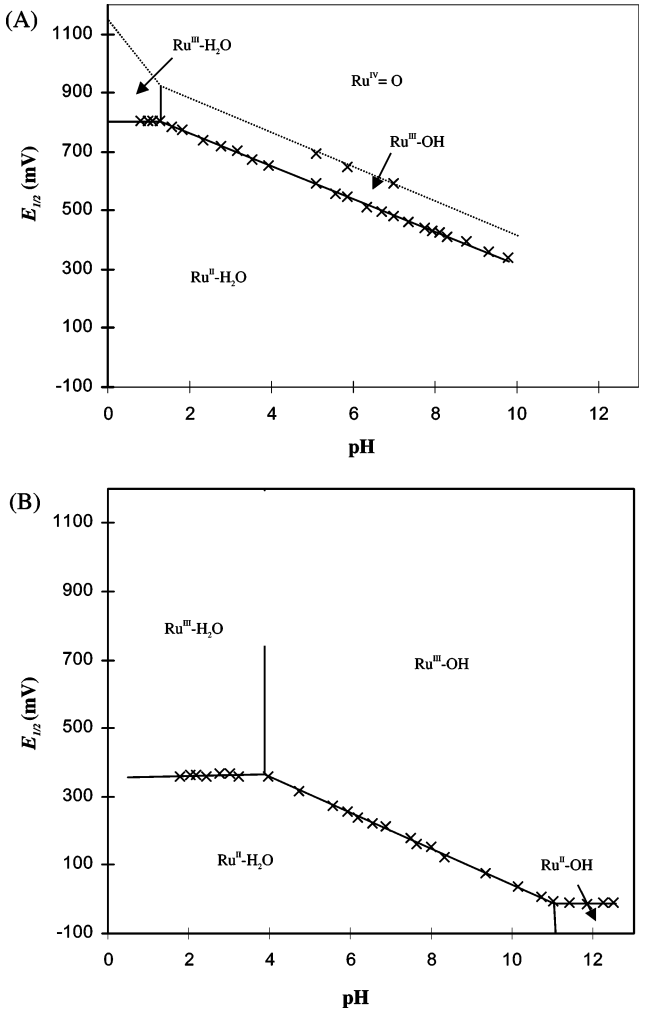

Figure 3. $E_{1/2}$ vs pH or Pourbaix diagram of complex: (A) **3mc**; (B) **3mo**. The pH-potential regions of stability for the various oxidation states and their dominant proton compositions are indicated.

Reactivity of Ru−O Species. Several reports have appeared in the literature dealing with the capacity of Ru−oxazoline complexes to carry out epoxidation reactions in a

(28) (a) Llobet, A. *Inorg. Chim. Acta* **1994**, *221*, 125. (b) Dovletoglou, A.; Adeyemi, S. A.; Meyer, T. J. *Inorg. Chem.* **1996**, *35*, 4120.
(29) (a) Leising, R. A.; Takeuchi, K. J. *Inorg. Chem.* **1987**, *26*, 4391. (b) Bessel, C. A.; Leising, R. A.; Takeuchi, K. J. *J. Chem. Soc., Chem. Commun.* **1991**, 883.

Table 4. Catalytic Oxidation of TS by Ru−Aqua Complexes Using $PhI(OAc)_2$ as the Oxidant[a]

entry	catalyst	TSO, %	BzA, %	ratio TSO/BzA	conv[b]
1	**3mo**	12.5	5.9	2.1	15.5
2	**3mc**	13.5	5.6	2.4	16.3
3	**3fo**	33.2	2.7	12.3	34.5
4	**3fc**	61.0	15.7	3.9	68.9

[a] Reaction conditions: catalytic oxidations were performed by dissolving the Ru−aqua complex (0.002 mmol) in degassed dichloromethane (2.5 mL) containing TS (0.2 mmol) and $PhI(OAc)_2$ (0.4 mmol). The reaction mixture was stirred at room temperature for 24 h. After the addition of an internal standard, an aliquot was taken for GC analysis. [b] Assuming that two molecules of BzA come from the scission of a single stilbene molecule.

catalytic manner with relatively good conversion yields.[22,30] However, it is difficult to compare these results with those of complexes **3** because the catalysts and oxidants used are substantially different. In the present paper, we report the catalytic activity of Ru−aqua precursor complexes **3mc**, **3mo**, **3fc**, and **3fo** with regard to their aptitude to epoxidize TS using $PhI(OAc)_2$ as the oxidant (see Table 4). A first glance at this table shows that in all cases the main product formed is *trans*-stilbene oxide (TSO) with minor amounts of benzaldehyde (BzA). It is also clear that the catalysts bearing the facial tpm ligand are much more active than those containing the meridional trpy. Entries 1 and 2 show that the **3mo** and **3mc** catalysts have a relatively similar performance regarding the oxidation of TS under similar conditions. From a geometrical viewpoint, the accessibility of the Ru═O active group toward the substrate in **3mo** and **3mc** is exactly the same because of the trans nature of the **3mo** isomer (see Figure 1). On the other hand, electronically they are substantially different because their $Ru^{III/II}$ redox couples differ by 280 mV (see Table 3). Therefore, one can infer from this that for this particular oxidation the electronic nature of the Ru═O active group does not practically affect the reactivity. Furthermore, the fact that for complex **3fo**, with a relatively similar redox potential as **3mo** (they differ by only 30 mV) but with a facial ligand instead of a meridional ligand, the catalyst performance strongly increases clearly points out that the main factor governing the reactivity is of a geometrical nature. The different reactivities for the two facial catalyst precursors, **3fc** and **3fo**, could be explained in terms of π-stacking effects. As shown in the X-ray structure for the corresponding Ru−Cl complex **2fc** (Figure 1A), the C15−C20 oxazolinic aromatic phenyl group situated parallel to the equatorial plane in complex **3fc** could have a reasonable contact with the aromatic system of the TS substrate when interacting with the Ru═O group. On the other hand, for the **3fo** complex, the free rotation around the C−N bond makes a similar π-stacking type of interaction highly unlikely. This type of π-stacking interaction would also be very unlikely with the meridional **3mc** and **3mo** because their benzylic aromatic rings are nearly perpendicular to the equatorial plane.

Acknowledgment. This research has been financed by the MCYT of Spain through Projects BQU2003-02884, BQU2006-15634, CSD2006-0003, and CTQ2004-01546/BQU. A.L. and I.R. thank Johnson and Matthey Ltd. for a $RuCl_3 \cdot xH_2O$ loan. X.S. is grateful for the award of a doctoral grant from the University of Girona.

Supporting Information Available: Additional crystallographic, spectroscopic, and electrochemical data. This material is available free of charge via Internet at http://pubs.acs.org.

IC070087Q

(30) Bennett, S.; Brown, S. M.; Conole, G.; Kessler, M.; Rowling, S.; Sinn, E.; Woodward, S. *J. Chem. Soc., Dalton Trans.* **1995**, *3*, 367.